

# Benzene hydrogenation over Ni/Al<sub>2</sub>O<sub>3</sub> catalysts prepared by conventional and sol–gel techniques

P.G. Savva <sup>a,1</sup>, K. Goundani <sup>a</sup>, J. Vakros <sup>a</sup>, K. Bourikas <sup>a</sup>, Ch. Fountzoula <sup>b</sup>,  
D. Vattis <sup>b</sup>, A. Lycourghiotis <sup>a</sup>, Ch. Kordulis <sup>a,\*</sup>

<sup>a</sup> University of Patras, Department of Chemistry, GR 265 00, Patras, Greece

<sup>b</sup> Technological Education Institute of Athens, Faculty of Technological Applications, Department of Physics, Chemistry and Materials Technology, Ag. Spyridonos Street, GR 122 10 Egaleo, Athens, Greece

Received 14 September 2007; received in revised form 17 October 2007; accepted 21 October 2007

Available online 26 October 2007

## Abstract

Nickel supported on alumina catalysts have been prepared using various synthesis methods (dry impregnation, co-precipitation, sol–gel) and evaluated for the hydrogenation of benzene contained in gasoline. The evaluation was carried out in a laboratory scale high pressure fixed bed reactor fed with a stream of surrogated reformate gasoline consisted by a mixture of hexane, benzene and toluene. All catalysts have been characterized by the joint use of various physicochemical characterization methods (XRF, BET, TGA, SEM, XRD, UV–vis DRS and XPS) in order to correlate their catalytic performances to their physicochemical properties. The results obtained revealed that sol–gel procedure, especially when it is followed by supercritical drying (aerogel), produced the most promising catalysts for the aforementioned catalytic process. Sol–gel methodology ensured the best compromise between dispersion of the nickel phase and its interaction with the support surface. Co-precipitated catalysts exhibited important activities but lower than those of the sol–gel catalysts. The catalyst prepared by dry impregnation proved to be the less active. Calcination of the catalysts before their activation by reduction decreased their activities.

© 2007 Elsevier B.V. All rights reserved.

**Keywords:** Benzene reduction; Hydrogenation; Gasoline; Catalyst preparation; Nickel supported on alumina; Sol–gel; Aerogel

## 1. Introduction

The hydrogenation of benzene is of major importance in the refineries due to the stringent environmental regulations governing its concentration in diesel fuels [1,2]. A large portion (70–80%) of benzene entering the motor gasoline pool is produced during catalytic reforming. Fractionation of the reformate gasoline and the subsequent hydrogenation of the fraction reach in benzene avoids high consumption of hydrogen and drastic reduction of the octane number in the final gasoline pool produced after remixing of the two fractions [3–5]. Following this route reformate gasoline with benzene concentration meeting the environmental regulations is obtained.

A large number of catalysts reported in the open literature may be used in the benzene hydrogenation. (e.g. Pt/mordenites [6], Ni/MCM-41 [7,8], Ru/SiO<sub>2</sub>, Ru/TiO<sub>2</sub>, RuFe/TiO<sub>2</sub>, RuFe/SiO<sub>2</sub> [9], Ni/SiO<sub>2</sub> [10], NiB/bentonite [11], Ir/γ-Al<sub>2</sub>O<sub>3</sub> [12], Pt/LTL and Pt/MOR zeolites [13], Ru/γ-Al<sub>2</sub>O<sub>3</sub> [14], Ni/Al-pillared clays [15,16], Ni/SiO<sub>2</sub>–Al<sub>2</sub>O<sub>3</sub> [17–21]. Among these, nickel supported catalysts are currently used in industry [22]. The choice of nickel is mainly due to its availability and reasonable cost compared to noble metals. The industrial catalysts very often contain high percentage of nickel supported on various oxides [15].

It has been found that the activity of the nickel catalysts for the title reaction depends on various parameters. One of them is the nature of the support as it may affect the properties of the active phase. On the other hand the aforementioned activity depends on the dispersion and the reducibility of the active phase as well as on the supported phase-support interactions. For a given support these characteristics depend on many parameters such as the preparation method, the pre-treatment

\* Corresponding author. Tel.: +30 2610 997 125; fax: +30 2610 994 796.

E-mail address: [kordulis@chemistry.upatras.gr](mailto:kordulis@chemistry.upatras.gr) (C. Kordulis).

<sup>1</sup> Present address: Department of Chemistry, University of Cyprus, P.O. Box 20537, CY1678 Nicosia, Cyprus, Tel.: +357 22 892772; fax: +357 22 892801.

steps (drying and calcination), and the conditions of the reduction (temperature, heating rate and space velocity of reducing stream) [8].

In order to achieve high activity, many researchers have focused on the development of high surface area nickel-alumina ( $\text{Ni}/\text{Al}_2\text{O}_3$ ) catalysts [23–26]. In this context a variety of preparation methods, such as deposition of nickel on high surface area alumina supports [27–35], nickel–alumina co-precipitation [34,36–42], and sol–gel methods [23,34] have also been studied. The latter has recently gained the interest of several researchers because it results to more homogeneous and more divided solids [19,43]. Moreover, it is reported that the sol–gel prepared supported metal catalysts and catalysts supports exhibit higher thermal stability, higher resistance to deactivation while allow a better flexibility in controlling catalyst properties such as particle size, surface area and pore size distribution [44]. Many authors report the sol–gel route as the best way to disperse catalytic metals on gels of fine texture [45].

Studies concerning the benzene hydrogenation are usually performed using pure benzene, in the absence of a solvent, though refineries treat aromatic feeds in hydrocarbon mixtures. In several works the simultaneous hydrogenation of various aromatics, which are competitively adsorbed on the active sites of the catalyst, is also studied [12,17,18,46]. However, the feed in a real dearomatization unit contains typically 10–40% of aromatic compounds, while the rest consists mainly of alkanes, cycloalkanes and alkenes [47,48].

In the present study we have investigated the influence of the preparation method on the physicochemical characteristics of  $\text{Ni}/\text{Al}_2\text{O}_3$  catalysts and thus on their activity for the complete hydrogenation of benzene under high pressure adopting a more realistic approach, namely using a surrogated reformate gasoline [49]. Specifically, three different preparation methodologies were compared: dry impregnation, co-precipitation and sol–gel. In the context of a particular preparation methodology we have also studied the influence of drying, calcination and nickel loading on the physicochemical characteristics and catalytic activity.

## 2. Experimental

### 2.1. Catalyst preparation

#### 2.1.1. Dry impregnation

A  $\text{Ni}/\text{Al}_2\text{O}_3$  catalyst containing 56 wt.% of nickel was prepared by dry impregnation. To be specific, an amount of  $\gamma\text{-Al}_2\text{O}_3$  powder (Akzo, SSA = 264  $\text{m}^2\text{ g}^{-1}$ , pore volume: 0.65  $\text{cm}^3\text{ g}^{-1}$ , 90–150 mesh) was washed with distilled water and dried at 120 °C overnight. A weighted amount of this powder was then impregnated in an aqueous solution of  $\text{Ni}(\text{NO}_3)_2\cdot 6\text{H}_2\text{O}$  (Merck, 99%) of a volume equal to its pore volume. The solution was added to the support under vigorous stirring at room temperature. The resulting impregnated solid was dried in air at 120 °C for 3 h. The so prepared catalyst will be referred as DI.

#### 2.1.2. Co-precipitation

Two catalysts containing also 56 wt.% Ni were prepared following co-precipitation at constant pH [50]. The required volumes of 0.5 M of nickel nitrate ( $\text{Ni}(\text{NO}_3)_2\cdot 6\text{H}_2\text{O}$  Merck, 99%) and aluminum nitrate (Merck, >98%) solutions were mixed in a separation funnel. The resulting solution was added drop-wise in a beaker containing 200 mL of distilled water under continuous stirring. The pH in the beaker was regulated at 8 using concentrated  $\text{NH}_4\text{OH}$  solution (Merck, 28%) and a pH stabilization system (Metrohm). A green hydroxide precipitate was formed. The precipitate was aged in the mother liquor overnight at 80 °C. Then, it was filtered and washed thoroughly until it was free of nitrates. It was then dried in an oven at 120 °C for 20 h. The resulted catalyst will be denoted as CP. An aliquot of this sample was calcined at 500 °C in static air for 20 h and this will be notified as CP-C.

#### 2.1.3. Sol–gel

Five  $\text{Ni}/\gamma\text{-Al}_2\text{O}_3$  catalysts were prepared by sol–gel. Specifically, the following procedure has been adopted [23]: 10 mmol of aluminum tri-sec-butoxide (Merck, 97%) was dissolved in 150 mmol of isopropanol (Merck, 99%) and then 5 mmol of acetylacetone (Merck, 99%) was added as a chelating agent under a nitrogen atmosphere. The precursor solution was vigorously stirred at room temperature for 30 min. The appropriate amount of nickel nitrate pre-dissolved in 60 mmol of deionized water was added drop-wise under mild stirring. A transparent green gel was formed in few minutes. The resulting gel was aged-dried for 5 days at room temperature. Using this procedure, two samples containing 10 and 15 wt.% Ni were prepared. These will be notified as SG-10 and SG-15, respectively. After removing an aliquot from the SG-10 sample the rest portion as well as the sample SG-15 were dried at 60 °C for another 5 days. Thus the samples SG-10-X and SG-15-X were prepared (X stands for xerogel). An aliquot from each of these samples was calcined at 600 °C for 5 h and the resulted samples will be notified as SG-10-X-C and SG-15-X-C, respectively. The solution entrapped in the removed from the SG-10 sample aliquot was extracted with liquid  $\text{CO}_2$ . During this process conditions above critical state of  $\text{CO}_2$  ( $T_C = 31.1\text{ }^\circ\text{C}$ ,  $P_C = 7.36\text{ MPa}$ ) had been applied. For this purpose, the gel was put in an autoclave, which was then completely filled with ethanol in order to minimize the evaporation of the solvent from the aerogel and to avoid the cracks during pressure build up. After the autoclave was heated to 40 °C,  $\text{CO}_2$  was pumped into the extractor to the pressure of 10 MPa. Before entering the extraction,  $\text{CO}_2$  was heated to the temperature of 40 °C. At the end of the extraction, the pressure was slowly released ( $\Delta P/\Delta t = 3\text{ bar/min}$ ) to atmospheric pressure. Thus, the SG-10-A sample was prepared (A stands for aerogel).

### 2.2. Catalyst activation

The samples prepared were reduced under pure  $\text{H}_2$  (40  $\text{mL min}^{-1}$ ) at 400 °C and atmospheric pressure for 20 h and then they reserved in a desiccator. The catalysts prepared

Table 1

The catalysts prepared, their Ni loading, their specific surface area (SSA), their % Ni atomic surface concentration ( $Ni_{sa}$ ), their wt.% Ni in the surface layer analyzed by XPS ( $Ni_{sw}$ ) and the binding energies (BE) of the Ni  $2p_{3/2}$  electrons

Catalyst	Ni loading (% w/w)	SSA ( $m^2 g^{-1}$ )	$Ni_{sa}$ (% atoms)	$Ni_{sw}$ (wt.%)	BE (Ni $2p_{3/2}$ )
DI	56.5	35	25.8	68.5	857.6
CP	56.0	188	2.2	6.2	857.2
CP-C	56.0	153	13.7	41.2	857.2
SG-10-X	10.7	271	1.7	4.1	857.5
SG-10-X-C	10.7	137	3.3	9.2	858.0
SG-10-A	10.7	329	—	—	—
SG-15-X	14.6	371	2.1	5.4	856.9
SG-15-X-C	14.6	195	4.2	11.5	857.1

and their loadings (measured by XRF) are compiled in Table 1. Only the dry impregnation and co-precipitation techniques allowed the preparation of Ni/Al<sub>2</sub>O<sub>3</sub> catalysts with Ni loading as high as that of the industrial catalysts [15]. Following the sol–gel methodology used in the present work it was difficult to achieve a loading higher than 15 wt.%. In those cases the gelation was difficult and the initially formed gel, if any, was not stable.

### 2.3. Catalyst characterization

X-ray diffraction (XRD) measurements of the samples were carried out on a Philips PW/1830 diffractometer using nickel-filtered Cu K $\alpha$  radiation ( $\lambda = 1.54 \text{ \AA}$ ).

Scanning electron microscopy (SEM) photographs were taken using a JEOL 6300 microscope. The samples studied were covered with a thin film of gold (ion sputtering). The voltage used was 25 kV, the intensity of the current used was 0.1–10 nA and the samples were exposed to the electron beam for 70 s.

BET surface areas of the samples were determined using nitrogen physisorption.

The UV–vis diffuse reflectance spectra of the catalysts were recorded using a Varian, (Cary 1/3) spectrophotometer in the wavelength range of 200–800 nm.

The X-ray photoelectron (XPS) spectra of the catalysts were recorded in an UHV chamber at a residual pressure of  $10^{-8} \text{ mbar}$  (1 mbar = 100 Pa). The latter was equipped with a hemispherical electron energy analyzer (SPECS, LH 10) and a twin-anode X-ray gun for XPS [51].

The thermogravimetric analysis (TGA) of the samples was carried out in a He atmosphere using a Dupont thermo-balance. In all experiments the sample temperature was increased from 25 to 600 °C using a heating rate of 10 °C min<sup>-1</sup>.

X-ray fluorescence (XRF) spectra were recorded with a Spectrace Instruments (QuanX/LN) spectrometer using a Pd excitation filter (0.025 mm thickness) and a current of 15 kV (0.08 mA).

### 2.4. Catalytic tests

The gas phase hydrogenation of benzene to cyclohexane was carried out in a high pressure fixed bed reactor described previously [49]. 300 or 500 mg of catalyst mixed with 3 mL of

quartz were used ( $90 \mu\text{m} \leq d_p \leq 150 \mu\text{m}$ ) in all catalytic experiments. The catalyst was pretreated with He at 25 °C for 30 min. The feed was then switched to pure H<sub>2</sub> (500 mL min<sup>-1</sup>), the pressure was raised up to 50 atm (1 atm = 101,325 Pa) and the temperature was set to 350 °C for 1 h [52]. The temperature was then reduced to 210 °C and a stream of surrogated reformate gasoline was added in the reactor inlet (0.25 mL min<sup>-1</sup>) for 5 h. This surrogated gasoline was consisted of 80.9 wt.% *n*-hexane (Merck, extra pure, 99%, MB = 86.18 g/mol), 14.9 wt.% benzene (Merck, 99.7%, MB = 78.11 g/mol) and 4.2 wt.% toluene (Merck, 99.5%, MB = 92.14 g/mol). The liquid effluent of the reactor was collected in half hour intervals and quantitatively analyzed by a gas chromatograph (GC-8A, Shimadzu) equipped with a flame ionization detector (FID) and a capillary column (wide bore fused silica column 25 m × 0.53 mm CP-Sil 5 CB, Chrompack). Cyclohexane and methyl cyclohexane were the only products of benzene and toluene hydrogenation detected, respectively. The procedure described was repeated for the temperatures 120, 150, 180 and again 210 °C for confirmation. All the tested catalysts remained at each reaction temperature for 5 h and their activity remained constant for the last three hours. No change in the activity was observed between the first and the last catalytic run at 210 °C, indicating that no deactivation of the catalysts took place during the whole catalytic test. Experiments performed with various catalyst masses (*W*) and gasoline flow rates (*F*) (keeping constant the ratio (*W/F*)) as well as on various catalyst particle sizes (keeping constant the catalyst mass) proved that the catalytic process was under kinetic control.

## 3. Results

### 3.1. Catalyst characterization in the oxide state

#### 3.1.1. Thermogravimetric analysis

The thermogravimetric analysis of the dried samples was performed in the temperature range 50–600 °C. Fig. 1A illustrates the TGA curves of the DI and CP samples as well as those of a Ni(NO<sub>3</sub>)<sub>2</sub>·6H<sub>2</sub>O–γ-Al<sub>2</sub>O<sub>3</sub> mechanical mixture (MM) and Ni(OH)<sub>2</sub>. Inspection of this figure reveals a similarity between the TGA curves of DI and MM samples as well as between those of the Ni(OH)<sub>2</sub> and the CP samples. These similarities rather suggest that in the DI sample nickel is

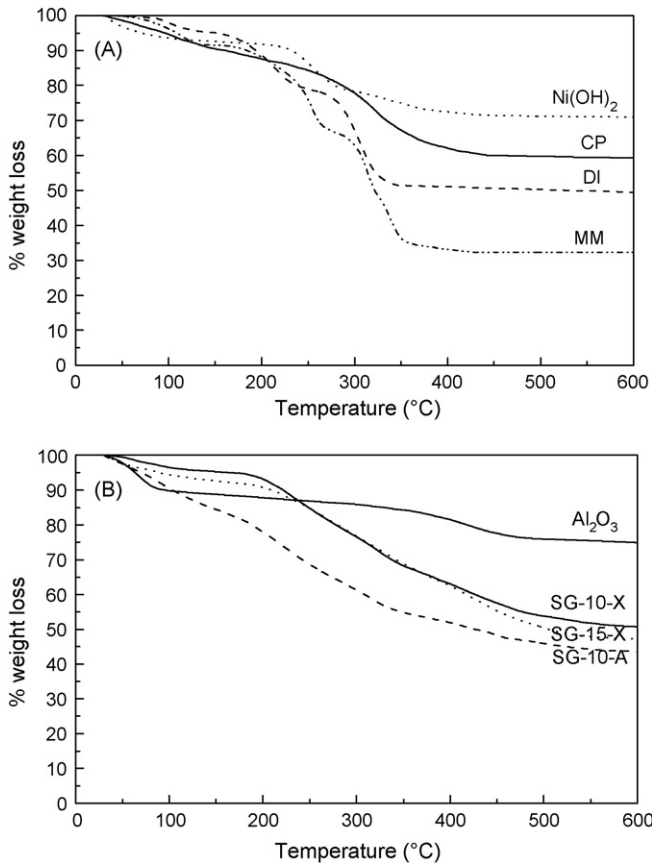


Fig. 1. (A) TGA curves of the dried DI and CP samples, of a  $\text{Ni}(\text{NO}_3)_2 \cdot 6\text{H}_2\text{O}$ – $\gamma\text{-Al}_2\text{O}_3$  mechanical mixture (MM) and  $\text{Ni}(\text{OH})_2$ . (B) TGA curves of the dried sol–gel samples and of dried pure alumina prepared by the same method.

deposited mainly in the form of corresponding nitrate salt by bulk precipitation [53] whereas  $\text{Ni}(\text{OH})_2$  and  $\text{Al}(\text{OH})_3$  are the predominant phases in the case of CP sample.

The TGA curves of the samples prepared by sol–gel are illustrated in Fig. 1B. The TGA curve of pure alumina prepared by the same method is also presented. These curves show that the removal of physisorbed water is completed up to 150 °C (with the exception of the SG-10-A sample from which the removal of physisorbed water is completed at about 200 °C). The weight loss observed in the temperature range 190–360 °C could be attributed to the decomposition of nitrates entrapped in the narrow pores of the Ni containing xero- and aerogels. Finally, the weight loss observed at temperatures higher than 360 °C in all samples should be attributed to the removal of structural water from the alumina.

### 3.1.2. DRS study

Fig. 2 presents the DR spectra of the DI (a) and CP (b) samples after drying and that of the CP-C (c) after calcination. The spectra of a  $\text{Ni}(\text{NO}_3)_2 \cdot 6\text{H}_2\text{O}$ – $\text{Al}_2\text{O}_3$  mechanical mixture (MM) containing the same Ni percentage (d), the  $\text{NiO}$  (e), the  $\text{NiAl}_2\text{O}_4$  (f) and the  $\text{Ni}(\text{OH})_2$  (g) are also included for comparison. The features of the reference compounds spectra are in very good agreement with those described in the literature [54,55]. The similarity between the spectra (a) and (d)

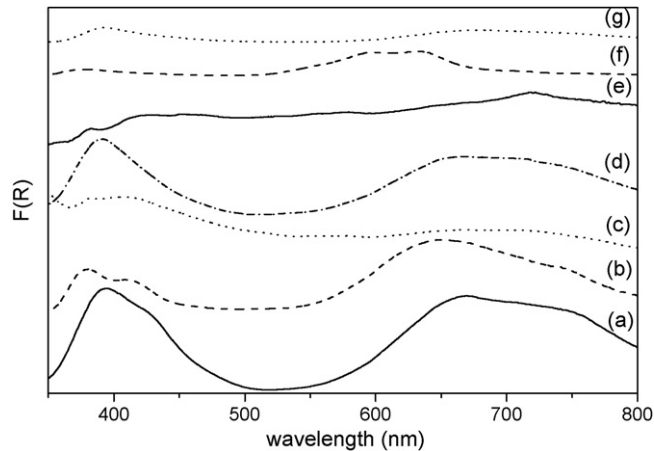


Fig. 2. DR spectra of the DI (a) and CP (b) samples after drying, of the CP-C (c) after calcination, of a  $\text{Ni}(\text{NO}_3)_2 \cdot 6\text{H}_2\text{O}$ – $\text{Al}_2\text{O}_3$  mechanical mixture (MM) containing the same Ni percentage (d), of the  $\text{NiO}$  (e), of the  $\text{NiAl}_2\text{O}_4$  (f) and of the  $\text{Ni}(\text{OH})_2$  (g).

confirmed the TGA finding that in the DI sample the Ni is deposited by bulk precipitation of the nitrate salt. The shoulder observed in the spectrum (a) at ca 420 nm could be considered as an indication that some  $\text{NiO}$  is also formed upon drying of the DI sample.

On the other hand, comparison of the spectrum (b) with the spectrum (g) reveals that Ni presumably precipitates as  $\text{Ni}(\text{OH})_2$  in the CP sample in agreement with the TGA results. However, the formation of small amount of  $\text{NiO}$  upon drying of this sample cannot be excluded taking into consideration the absorbance observed at ca. 420 nm. Calcination of the CP sample brings about the transformation of the  $\text{Ni}(\text{OH})_2$  mainly into  $\text{NiO}$  and not  $\text{NiAl}_2\text{O}_4$ . This is confirmed by the very good similarity between the spectra (c) and (e).

Finally, the DR spectra of the samples prepared by sol–gel (not presented) revealed that nickel is entrapped mainly as  $\text{Ni}(\text{NO}_3)_2$  into alumina pores. Some evidence also exist that the  $\text{Ni}(\text{NO}_3)_2$  crystallites formed in the case of SG-10-A sample are smaller than those of the SG-10-X sample.

## 3.2. Catalyst characterization in the final reduced state

### 3.2.1. Texture

The specific surface areas (SSAs) of the catalysts studied are presented in Table 1. Inspection of this table shows that the catalysts prepared following the sol–gel methodology exhibited relatively high SSAs. Their values increase with the Ni loading and decrease remarkably when the samples undergo calcination before reduction. It should be also stressed the favorable influence on the SSA of the supercritical drying. It is well known that elimination of the solvent from the gel, under ambient conditions, results in a large shrinkage [56]. This does not matter for the preparation of dense glassy material, but if one wants to keep the highly porous network of the wet gel, other methods of drying have to be employed, such as that with supercritical fluids applied in our case. Aerogels in the form of simple or mixed oxides exhibit high surface areas and large pore volumes [57].

The catalysts prepared by co-precipitation exhibited higher SSAs than that of the impregnated catalyst but lower than those of the sol-gel ones. However, the calcination of the co-precipitated catalyst provoked also significant diminution of its SSA.

### 3.2.2. Morphology

Stereographic pictures of the final catalysts taken from a scanning electron microscope showed a shrinkage provoked by the calcination performed before the reduction of the samples. See for example Fig. 3 where the SEM photographs of the CP (Fig. 3A) and CP-C (Fig. 3B) are presented. This shrinkage was independent of the preparation methodology used and the Ni content of the samples. It explains why the SSAs of the calcined samples are lower than those of the corresponding non-calcined ones.

### 3.2.3. Catalyst structure

The XRD patterns of the SG samples (not presented) appeared very low and broad peaks indicating that all these catalysts were almost amorphous materials. This is in agreement with the high surface areas exhibited by these samples. Fig. 4 presents the XRD patterns of the DI, CP and

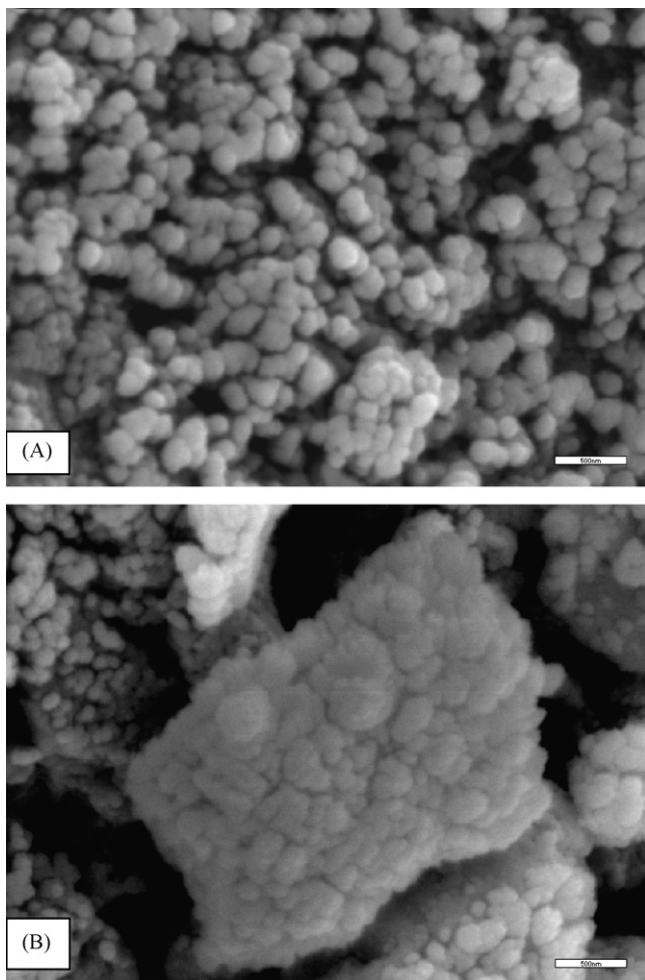


Fig. 3. SEM photographs of the reduced CP (A) and CP-C (B) samples (scale: 500 nm).

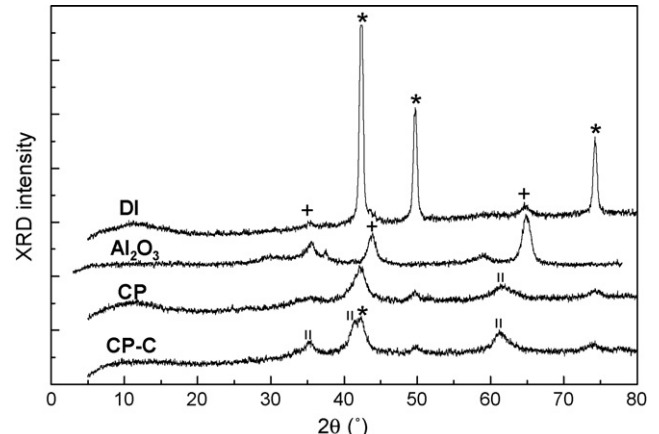


Fig. 4. XRD patterns of the reduced DI, CP, CP-C catalysts and that of the alumina used as carrier in the DI catalyst. (\*) Metallic Ni, (+)  $\gamma$ -Al<sub>2</sub>O<sub>3</sub>, (||) NiO.

CP-C catalysts as well as that of the alumina used as carrier in the DI catalyst.

The narrow and very intensive peaks detected in the XRD pattern of the DI catalyst reveal that metallic nickel is the predominant crystal phase in this catalyst. The high crystallinity of the supported nickel is in very good agreement with the low surface area of this catalyst. In contrast, the XRD patterns of the co-precipitated catalysts show that a significant fraction of nickel oxide, besides of the metallic nickel, is also present in these samples after reduction. This fraction seems to be higher in the CP-C sample. The existence of the non-reduced nickel phase reveals that a strong interaction is exerted between the relatively well dispersed nickel phases and the co-precipitated alumina. However, the corresponding XRD peaks are less intensive and wider than those observed in the case of the DI catalyst. This shows a lower crystallinity of the nickel phases formed by the thermal and activation (reduction) treatments which followed co-precipitation. Finally, the XRD peaks of the nickel phases in the CP-C sample are more intensive and have smaller full width at their half maximum than the corresponding peaks in the XRD pattern of the CP sample. This shows that calcination of the co-precipitated sample provoked diminution in the dispersion of the nickel phase.

### 3.2.4. XPS surface characterization

The values of the binding energy of the Ni 2p<sub>3/2</sub> core electrons for the catalysts studied are compiled in Table 1. Fig. 5 shows the XP spectrum of the Ni 2p core level for the CP-C catalyst which is representative for all the catalysts studied. A major peak appears at ca. 857.2 eV corresponding to Ni 2p<sub>3/2</sub> photoelectrons. The position of this peak as well as the appearance of the satellite lines in its spectral region are related to non-fully reduced nickel ions interacting with the alumina surface [58,59]. These results show that the nickel being in the surface layer analyzed by XPS is probably re-oxidized upon the transfer of the samples to the XPS machine. As no re-reduction took place in situ, it is not possible on the base of the XPS to draw conclusions concerning the influence of the preparation method on the reducibility of the supported nickel.

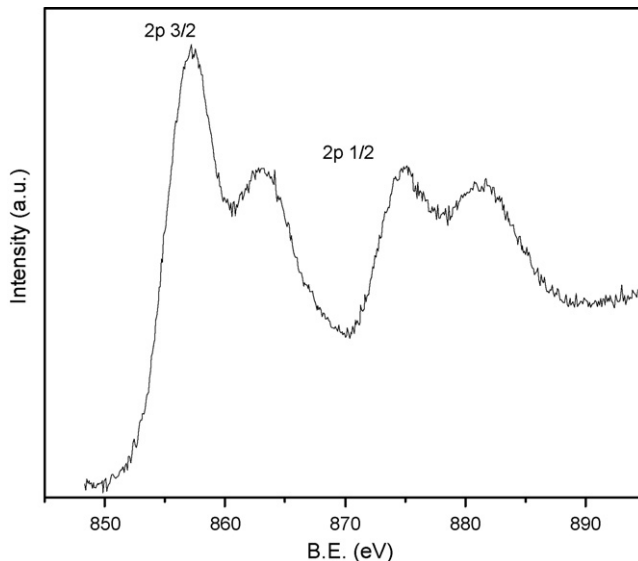


Fig. 5. X-ray photoelectron spectrum of the of Ni 2p core level for the reduced CP-C catalyst.

The XPS analysis of the samples permits the calculation of the percentage nickel atomic surface concentrations ( $Ni_{sa}$ ) as well as the percentage weight nickel concentration (wt.% Ni ( $Ni_{sw}$ )) in the surface layer analyzed by XPS. The calculated values are summarized in Table 1. These values show that with the exception of the DI catalyst all the non-calcined samples exhibited very low nickel surface concentrations, even lower than their bulk composition. This probably indicates that the nickel phase is encapsulated inside the alumina pores in all these samples. On the contrary, in the case of the DI catalyst the main part of the nickel phase seems to be deposited on the external surface of the alumina. The calcination of the CP and SG samples provoked a surface enrichment by the nickel phase approaching the corresponding bulk composition. This is probably due to the thermal sintering of the alumina bringing about a pore opening and a surface area decrease in accordance with the BET results presented above.

### 3.3. Catalytic performance

The conversions of benzene to cyclohexane obtained over the high loaded DI and CP samples are presented in Fig. 6. The catalytic performances of these samples seem to be strongly depended on the preparation method and the pretreatment. The DI catalyst exhibited very low activity in the temperature range 120–210 °C. Unexpectedly, negligible increase in activity was observed over this catalyst as the temperature increased from 180 to 210 °C. On the other hand, the CP catalyst proved to be from 12 to 18 times more active than the DI one in the aforementioned temperature range. The calcination of the CP catalyst provoked a significant diminution of its hydrogenation activity.

Fig. 7 shows the conversions of benzene observed over the SG catalysts. The activity of these catalysts is strongly influenced by the details of the preparation procedure (the drying method, the Ni loading and the calcination). The

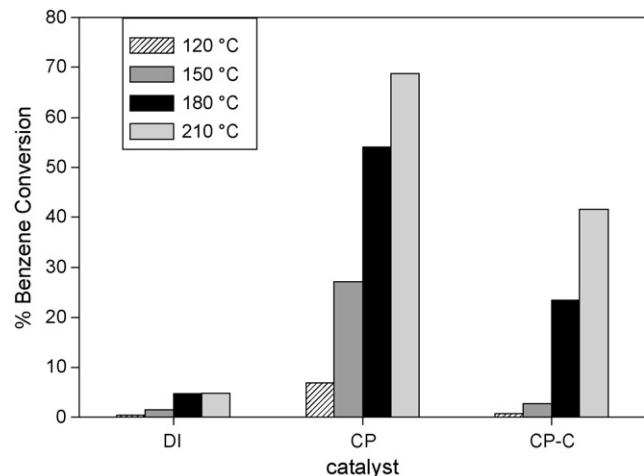


Fig. 6. The benzene conversion achieved over the high loaded DI, CP and CP-C samples, in the temperature range 120–210 °C ( $P = 50$  atm, liquid feed rate =  $0.25$  mL min $^{-1}$ , hydrogen feed rate =  $500$  mL min $^{-1}$ , mass of catalyst =  $300$  mg).

application of supercritical drying and the increase of the Ni loading caused a considerable increase in the catalytic activity. In contrast, the calcination of the xerogels before reduction brought about a decrease in the catalytic activity. This is more pronounced in the sample with the low Ni content.

Closing this section it should be noticed that the conversion of benzene observed in all cases was about four times higher than that of the toluene.

## 4. Discussion

In the following discussion we shall try to correlate the catalytic behavior of the  $Ni/Al_2O_3$  catalysts studied with their physicochemical characteristics. It is well known that the latter are governed by the preparation method and the details of the preparation procedure [53].

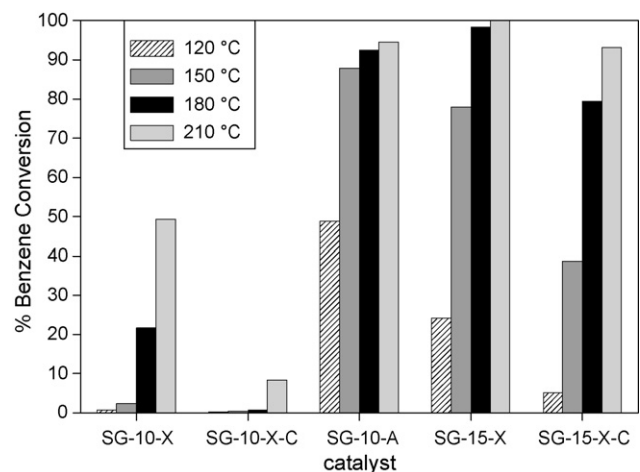


Fig. 7. The benzene conversion achieved over the SG catalysts in the temperature range 120–210 °C ( $P = 50$  atm, liquid feed rate =  $0.25$  mL min $^{-1}$ , hydrogen feed rate =  $500$  mL min $^{-1}$ , mass of catalyst =  $500$  mg).

Taking into account the specific surface areas of the catalysts involved in Table 1 as well as their activities presented in Figs. 6 and 7 one might conclude that this textural characteristic is probably one of the key factors for the benzene hydrogenation activity exhibited by the Ni/Al<sub>2</sub>O<sub>3</sub> catalysts studied.

However, comparing the high loaded catalysts (Fig. 6, Table 1) it is obvious that their activity is not determined only by their SSAs. Presumably, the relatively low crystallinity (relatively high dispersion) of the nickel phases achieved following the co-precipitation methodology is also responsible for the higher activities exhibited by these catalysts. The dependence of the activity on the dispersion of the nickel phase becomes even more pronounced by comparing the activities of the two co-precipitated samples. In fact, the calcination of the CP sample, which according to XRD results brought about a decrease in the dispersion of the nickel phase maintaining the NiO phase predominant (see also DRS results), provoked a 20% reduction in the specific surface area while the corresponding diminution in the catalytic activity ranged from 40 to 90%, depending on the reaction temperature.

On the other hand the high crystallinity (low dispersion) of the nickel phases observed on the DI catalyst should be considered to be responsible not only for the low activity of this catalyst but also for the creation of carbonaceous deposits on its surface [60]. The concentration of these deposits increases with the reaction temperature accelerating the deactivation of the corresponding catalyst. This effect might explain the unexpected negligible change of conversion with temperature over the DI sample (see Fig. 6).

As already mentioned the preparation method influences strongly the characteristics of the final catalyst [53]. It is well known that sol–gel derived alumina materials have high surface areas, controllable nano-particle size, and versatile structures [61–63]. Nickel/alumina catalysts prepared by sol–gel have a more stable support structure and higher nickel dispersion than those catalysts prepared by impregnation resulting thus in higher activity and resistance to carbon deposition [23,64,65]. Indeed, the sol–gel technique applied in this work for the preparation of the low loaded samples produced catalysts with high surface areas and well dispersed nickel phase. The reduction of these catalysts presumably resulted to the transformation of the Ni(NO<sub>3</sub>)<sub>2</sub> nano-crystals initially entrapped in the alumina pores (according to the DRS results) to very small metallic nickel nano-particles. Thus, the corresponding catalysts exhibited very high activities, especially, when the supercritical drying was followed.

The calcination of the SG samples before their activation (reduction) resulted to a decrease of their activity, as in the case of the CP sample. This general behavior of the Ni/Al<sub>2</sub>O<sub>3</sub> catalysts could be attributed to the sintering of active phase and the development of very strong interactions with the alumina surface (probable formation of inactive NiAl<sub>2</sub>O<sub>4</sub>) induced by calcination. However, Boudjahem et al. [66,67] have observed the opposite behavior in the case of the Ni/SiO<sub>2</sub> catalysts.

Although sintering of the nickel phase of the SG samples has not been detected at least by XRD, it might be provoked due to

the support surface area diminution. On the other hand, calcination of these samples may bring about an increase of interaction of nickel with alumina surface. In fact, the formation of well dispersed NiAl<sub>2</sub>O<sub>4</sub> could not be excluded. According to the literature the interaction between nickel and the alumina support is complex [42]. During preparation, Ni<sup>2+</sup> could disperse on the surface of Al<sub>2</sub>O<sub>3</sub>, or diffuse into the bulk structure of Al<sub>2</sub>O<sub>3</sub> to different extents, depending on the intrinsic properties of the support, nickel loading, and preparation parameters. Nickel can be highly dispersed on the surface if nickel is incorporated into the spinel structure of alumina to form NiAl<sub>2</sub>O<sub>4</sub>. The dispersion is maintained because of the strong interaction between Ni<sup>2+</sup> and the support. The Ni<sup>2+</sup> in NiAl<sub>2</sub>O<sub>4</sub>, however, is difficult to reduce at temperatures below approximately 700 °C [33,68] and, thus, may not be active for all reactions, depending on the reduction temperature. High temperature reductions tend to result in sintering. More weakly bound nickel species, such as nickel oxide (NiO), are easier to reduce but also more easily sintered, resulting in larger particles that promote carbon formation. Rather than being completely incorporated into the alumina structure, a surface nickel spinel phase may be also formed [54]. This phase is between bulk nickel aluminate and nickel oxide in terms of interaction with the support, and may be a suitable compromise with respect to reducibility and stability, but may also be more difficult to be produced. However, the sol–gel methodology followed in the present study seems to favor the formation of such a nickel phase.

As mentioned in the “Catalytic performance” section the conversion of benzene observed in all cases was about four times higher than that of the toluene. It is well known that the presence of toluene in the reaction mixture inhibits the benzene hydrogenation under high [49] and atmospheric pressure conditions [69–72]. In the most of cases the above behavior is attributed to the competitive adsorption of aromatics on the active sites. It is generally assumed that both molecules can be adsorbed by a π-bond interaction in which the ring lays parallel to the metal surface [70]. As a result of the inductive effect of the methyl group and therefore its higher π-electron cloud density, toluene is expected to be adsorbed more strongly than benzene on Group VIII metals [73]. Taking into account all the above, we can attribute the higher conversion of benzene observed over our catalysts to the relatively low toluene concentration in the surrogated gasoline used as feed.

In order to better evaluate the influence of the preparation method on the activity of the Ni/Al<sub>2</sub>O<sub>3</sub> catalysts for the benzene hydrogenation under high pressure, we have calculated the reaction rates achieved over the non-calcined samples, per mass of nickel contained in each catalyst. The calculation concerns the lowest reaction temperature examined by considering differential working mode for the reactor. These values are presented in Fig. 8. It is obvious that sol–gel is the most promising method for preparing Ni/Al<sub>2</sub>O<sub>3</sub> catalysts suitable for benzene hydrogenation in a gasoline fraction. In this point it should be noticed that the reaction rate obtained over the aerogel catalyst proved higher than that of a commercial Ni/

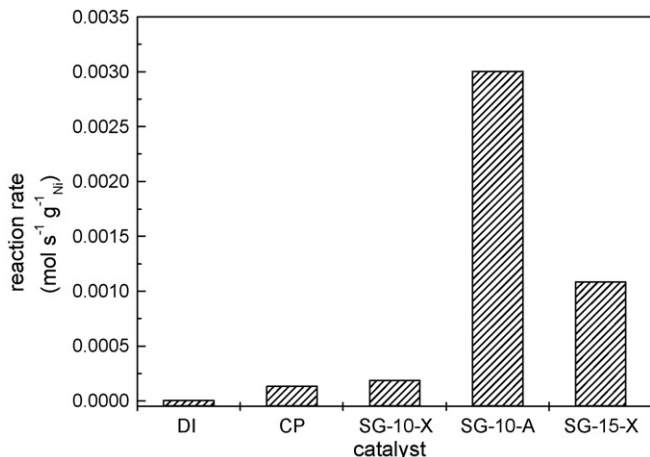


Fig. 8. The reaction rate achieved over the non-calcined samples, per gram of Ni, at 120 °C ( $P = 50$  atm, liquid feed rate = 0.25 mL min $^{-1}$ , hydrogen feed rate = 500 mL min $^{-1}$ ).

$\text{Al}_2\text{O}_3$  catalyst used for this reaction and tested under the same conditions [74].

This picture is in line with the aforesaid inference that the sol–gel methodology ensures better compromise between dispersion of nickel phase and its interaction with the support surface than co-precipitation and dry impregnation. The best compromise and thus the highest activity are achieved when the sol–gel preparation is followed by supercritical drying of the prepared gel.

## 5. Conclusions

The most important findings of the present study may be summarized as follows:

1. The sol–gel procedure for preparing Ni/ $\text{Al}_2\text{O}_3$  catalysts, especially when it is followed by supercritical drying, produces very promising catalysts for the hydrogenation of benzene involved in reformate gasoline.
2. The activity of these catalysts increases with the nickel loading. However, high nickel concentrations (>15 wt.% Ni in the final sample) in the sol prohibit its gelation.
3. The sol–gel methodology ensures better compromise between dispersion of nickel phase and its interaction with the support surface than co-precipitation and dry impregnation.
4. Calcination of the Ni/ $\text{Al}_2\text{O}_3$  catalysts before their activation by reduction decreases their activities for benzene hydrogenation. This decrease is due to the decrease of the dispersion of nickel and the increase of its interaction with the alumina surface presumably resulting to the formation of  $\text{NiAl}_2\text{O}_4$  like species.

## Acknowledgment

This work is co-funded by 75% from E.U. and 25% from the Greek Government under the framework of the Education and Initial Vocational Training Program – Archimedes.

## References

- [1] Official Journal of the European Communities, 13.12.2000, L 313/12–21.
- [2] R. Molina, G. Poncelet, *J. Catal.* 199 (2001) 162.
- [3] M.A. Arribas, F. Márquez, A. Martínez, *J. Catal.* 190 (2000) 309.
- [4] A. Stanislaus, B.H. Cooper, *Catal. Rev. Sci. Eng.* 36 (1994) 75.
- [5] A.R. Goelzer, A. Hernandez-Robinson, S. Ram, A.A. Chin, M.N. Harandi, C.M. Smith, *Oil Gas J.* 13 (1993) 63.
- [6] L.J. Simon, J.G. van Ommen, A. Jentys, J.A. Lercher, *Catal. Today* 73 (2002) 105.
- [7] A. Lewandowska, S. Monteverdi, M.M. Bettahar, M. Ziolek, *J. Mol. Catal. A* 3713 (2002) 1.
- [8] R. Wojcieszak, S. Monteverdi, M. Mercy, I. Nowak, M. Ziolek, M.M. Bettahar, *Appl. Catal. A* 268 (2004) 241.
- [9] J.W. da-Silva, A.J.G. Cobo, *Appl. Catal. A* 252 (2003) 9.
- [10] M.A. Ermakova, D.Yu. Ermakov, *Appl. Catal. A* 245 (2003) 277.
- [11] R. Zhang, F. Li, N. Zhang, Q. Shi, *Appl. Catal. A* 239 (2003) 17.
- [12] D.S. Cunha, G.M. Cruz, *Appl. Catal. A* 236 (2002) 55.
- [13] L.J. Simon, J.G. van Ommen, A. Jentys, J.A. Lercher, *J. Catal.* 201 (2001) 60.
- [14] C. Milone, G. Neri, A. Donato, M.G. Musolino, L. Mercadante, *J. Catal.* 159 (1996) 253.
- [15] A. Louloudi, N. Papayannakos, *Appl. Catal. A* 204 (2000) 167.
- [16] A. Louloudi, J. Michalopoulos, N.-H. Gangas, N. Papayannakos, *Appl. Catal. A* 242 (2003) 41.
- [17] V.L. Barrio, P.L. Arias, J.F. Cambra, M.B. Güemez, J.L.G. Fierro, *Appl. Catal. A* 242 (2003) 17.
- [18] B. Pawelec, P. Castano, J.M. Arandes, J. Bilbao, S. Thomas, M.A. Pena, J.L.G. Fierro, *Appl. Catal. A* 317 (2007) 20.
- [19] C. Guimon, A. Auroux, E. Romero, A. Monzon, *Appl. Catal. A* 251 (2003) 199.
- [20] V.L. Barrio, P.L. Arias, J.F. Cambra, M.B. Güemez, B. Pawelec, J.L.G. Fierro, *Catal. Commun.* 5 (2004) 173.
- [21] P. Castano, B. Pawelec, J.L.G. Fierro, J.M. Arandes, J. Bilbao, *Fuel* 86 (2007) 2262.
- [22] K. Weissermel, H.J. Arpe, *Industrial Organic Chemistry*, third ed., VCH, NY, 1997.
- [23] S. Tang, L. Ji, J. Lin, H.C. Zeng, K.L. Tan, K. Li, *J. Catal.* 194 (2000) 424.
- [24] T.V. Choudhary, C. Sivadinarayana, D.W. Goodman, *Chem. Eng. J.* 93 (2003) 69.
- [25] C.E. Quincoces, E.I. Basaldella, S.P. De Vargas, M.G. Gonzalez, *Mater. Lett.* 58 (2004) 272.
- [26] A. Valentini, N.L.V. Carreno, L.F.D. Probst, E.R. Leite, E. Longo, *Micro. Meso. Mater.* 68 (2004) 151.
- [27] Y.S. Oh, H.S. Roh, K.W. Jun, Y.S. Baek, *Int. J. Hydrogen Energy* 28 (2003) 1387.
- [28] S. Wang, G.Q.M. Lu, *Appl. Catal. B* 16 (1998) 269.
- [29] Z.X. Cheng, X.G. Zhao, J.L. Li, Q.M. Zhu, *Appl. Catal. A* 205 (2001) 31.
- [30] Z. Xu, Y. Li, J. Zhang, L. Chang, R. Zhou, Z. Duan, *Appl. Catal. A* 210 (2001) 45.
- [31] S. Takenaka, H. Ogihara, I. Yamanaka, K. Otsuka, *Appl. Catal. A* 217 (2001) 101.
- [32] C. Courson, L. Udras, C. Petit, A. Kienemann, *Sci. Tech. Adv. Mater.* 3 (2002) 271.
- [33] H.S. Roh, K.W. Jun, S.E. Park, *Appl. Catal. A* 251 (2003) 275.
- [34] A.I. Tsyganok, T. Tsunoda, S. Hamakawa, K. Suzuki, K. Takehira, T. Hayakawa, *J. Catal.* 213 (2003) 191.
- [35] J. Guo, H. Lou, H. Zhao, D. Chai, X. Zheng, *Appl. Catal. A* 273 (2004) 75.
- [36] J.-M. Wei, B.-Q. Xu, J.-L. Li, Z.-X. Cheng, Q.-M. Zhu, *Appl. Catal. A* 196 (2000) L167.
- [37] Y. Cesteros, P. Salagre, F. Medina, J.E. Sueiras, *Chem. Mater.* 12 (2000) 331.
- [38] T. Shishido, M. Sukenobu, H. Morioka, R. Furukawa, H. Shirahase, K. Takehira, *Catal. Lett.* 73 (2001) 21.
- [39] R. Villa, C. Cristiani, G. Groppi, L. Lietti, P. Forzatti, U. Cornaro, S. Rossini, *J. Mol. Catal. A* 204–205 (2003) 637.
- [40] Z. Hou, T. Yashima, *Appl. Catal. A* 261 (2004) 205.

[41] K. Takehira, T. Shishido, P. Wang, T. Kosaka, K. Takaki, *J. Catal.* 221 (2004) 43.

[42] G. Li, L. Hu, J.M. Hill, *Appl. Catal. A* 301 (2006) 16.

[43] C.J. Brinker, G.W. Scherer, *Sol-Gel Science*, Academic Press, NY, 1990.

[44] G. Goncalves, M.K. Lenzi, O.A.A. Santos, L.M.M. Jorge, *J. Non-Cryst. Solids* 352 (2006) 3697.

[45] J. Escobar, J.A. De Los Reyes, T. Viveros, *Appl. Catal. A* 253 (2003) 151.

[46] J.L. Rodriguez, E. Pastor, *Electrochim. Acta* 45 (2000) 4279.

[47] M.J. Girgis, B.C. Gates, *Ind. Eng. Chem. Res.* 30 (1991) 2021.

[48] P.A. Rautanen, J.R. Aittamaa, A.O.I. Krause, *Ind. Eng. Chem. Res.* 39 (2000) 4032.

[49] K. Goundani, Ch. Papadopoulou, Ch. Kordulis, *React. Kinet. Catal. Lett.* 82 (2004) 149.

[50] S. Narayanan, R. Unnikrishnan, V. Vishwanathan, *Appl. Catal. A* 129 (1995) 9.

[51] Ch. Kordulis, A.A. Lappas, Ch. Fountzoula, K. Drakaki, A. Lycourghiotis, I.A. Vasalos, *Appl. Catal. A* 209 (2001) 85.

[52] J.L. Margitfalvi, I. Kolosova, E. Tálas, S. Göbölös, *Appl. Catal. A* 154 (1997) L1.

[53] K. Bourikas, Ch. Kordulis, A. Lycourghiotis, *Catal. Rev.* 48 (2006) 363.

[54] M. Lo Jacono, M. Schiavello, A. Cimino, *J. Phys. Chem.* 75 (1971) 1044.

[55] E. Kis, R. Marinkovic-Neducin, G. Lomic, G. Boskovic, D.Z. Obadovic, J. Kiurski, P. Putanov, *Polyhedron* 17 (1998) 27.

[56] L.L. Hench, J.K. West, *Chem. Rev.* 90 (1990) 33.

[57] G.M. Pajonk, *Appl. Catal.* 72 (1991) 217.

[58] B. Pawelec, S. Damyanova, K. Arishtirova, J.L.G. Fierro, L. Petrov, *Appl. Catal. A* 323 (2007) 188.

[59] J. Moulder, W.F. Stickle, P.E. Sobol, K.D. Bomben, *Handbook of X-ray Photoelectron Spectroscopy*, second ed., Perkin-Elmer Corporation (Physical Electronics), 1992.

[60] D.L. Trimm, *Catal. Today* 49 (1999) 3.

[61] X. Bokhimi, J. Sanchez-Valente, F. Pedraza, *J. Solid State Chem.* 166 (2002) 182.

[62] U. Janosovits, G. Ziegler, U. Scharf, A. Wokaun, *J. Non-Cryst. Solids* 210 (1997) 1.

[63] F. Mange, D. Fauchadour, L. Barre, L. Normand, L. Rouleau, *Colloids Surf. A* 155 (1999) 199.

[64] Y. Zhang, G. Xiong, S. Sheng, W. Yang, *Catal. Today* 63 (2000) 517.

[65] J.-H. Kim, D.J. Suh, T.-J. Park, K.-L. Kim, *Appl. Catal. A* 197 (2000) 191.

[66] A.G. Boudjahem, S. Monteverdi, M. Mercy, D. Ghanbaja, M.M. Bettahar, *Catal. Lett.* 84 (2002) 115.

[67] A.G. Boudjahem, S. Monteverdi, M. Mercy, M.M. Bettahar, *J. Catal.* 221 (2004) 325.

[68] C. Li, Y.-W. Chen, *Thermochim. Acta* 256 (1995) 457.

[69] A.G.A. Ali, L.I. Ali, S.M. Aboul-Fotouh, A.K. Aboul-Gheit, *Appl. Catal. A* 170 (1998) 285.

[70] S.D. Lin, M.A. Vannice, *J. Catal.* 143 (1993) 539.

[71] T. Ioannides, X.E. Verykios, *J. Catal.* 143 (1993) 175.

[72] T. Ioannides, M. Tsapatsis, M. Kousathana, X.E. Verykios, *J. Catal.* 152 (1995) 331.

[73] M.C. Tsai, E.L. Muetterties, *J. Am. Chem. Soc.* 104 (1982) 2534.

[74] P. Savva, M.Sc. thesis, University of Patras, Patras, Greece, 2003.